EXPERIMENTAL AND NUMERICAL INVESTIGATION OF STRUCTURE-BORNE INTERIOR NOISE IN A SIMPLIFIED VEHICLE MODEL

VB Georgiev Department of Aeronautical and Automotive Engineering
RL Ranavaya Loughborough University
VV Krylov Loughborough, Leicestershire LE11 3TU, UK

1 INTRODUCTION

Structure-borne vehicle interior noise is one of the important refinement factors in automotive industry, and its mitigation leads to enhancement of consumers' perception of product's quality [1,2]. To reduce time and efforts required for analysing and mitigating vehicle interior noise, it is preferable to undertake most of the associated work on the design stage. The analysis of structure-borne interior noise can be carried out using different approaches. For a limited number of structures and cavities of simple geometry, one can use analytical solutions to structural-acoustic problems [3-5]. This provides a great opportunity for an explicit physical interpretation and understanding of the cases considered. In contrast to structures of simple geometry, irregular structures and cavities, such as real car compartments, can not be described analytically. In this case the conventional approach to predicting interior noise across entire frequency range relies upon synthesis of different modelling techniques. In the low frequency range, 10-250 Hz, the most common techniques are Finite Element Method (FEM) and Boundary Element Method (BEM), the upper frequency limit reported in literature being about 500 Hz [6-8]. In the high frequency range, above 500 Hz, Statistical Energy Analysis (SEA) is used widely.

Although the above-mentioned numerical methods, FEM and BEM, have achieved satisfactory levels of accuracy in predicting interior structural-acoustic response at low and medium frequencies, they are not much helpful in understanding physical mechanisms behind the problem that could assist in predicting the behaviour of similar but slightly modified vehicle structures. Therefore, there remains the scope for further development of the theory to assist in better understanding the physics of structure-borne interior noise, especially its dependence on different parameters of vehicle structures and interior cavities. In this case, a simplification of structural and acoustic models could be an attractive option to study the mechanisms of structure-born interior noise and to assist in better understanding the results of vibro-acoustic analysis.

The use of simplified and reduced scale models for theoretical and experimental investigations of structure-borne interior noise has been studied in the past by several researchers. In particular, purely acoustic experiments have been conducted on scale replicas of vehicle interiors with walls described by rigid boundary conditions [9,10]. In the example described by Lee *et. al.* [9], the model was a 1:2 scale replica of the passenger compartment of a saloon car. Gorman *et. al.* [10] simplified their models to equivalent rectangular cavities having the same volume as the actual enclosure in order to calculate the acoustic response. Most recently, the traditional structural-acoustic model – a simple rectangular cavity with one vibrating wall - was investigated again to demonstrate a new hybrid method for simulating the so-called 'boom noise' and identifying the parameters that affect its generation [11]. In addition to the above, some other types of simplified models have been considered for studying vehicle interior noise analytically and experimentally by two of the present authors and their colleagues [12-14].

The present study can be considered as further development of the above-mentioned philosophy by introducing simplified models of medium complexity. The main aim of such intermediate models is to bridge the existing large gap between the above-mentioned very simple analytical models and the very complex and detailed computer models currently used in automotive industry. For this

purpose, a new reduced-scale vehicle model of medium complexity has been built and tested experimentally and numerically. The experimental investigation included measurements of acoustic pressure frequency response functions (FRF's) at driver's and passenger's ear positions when an electromagnetic shaker was located at different places, thus simulating the disturbance from various sources. Along with the experimental investigation, a numerical study was carried out using finite element software - MSC.Nastran and MSC.Patran. Although this study is concerned with structure-borne vehicle interior noise, its results and conclusions could be of interest also for other branches of engineering, such as building acoustics and dynamics of thin shell structures.

2 MODEL DESCRIPTION AND EQUIPMENT

Although the developed vehicle model is rather irregular, it is still simple enough to enable studying the effects of different model parameters on structural-acoustic response and to proof the efficiency of some measures of reducing structure-born noise. The model consists of two main parts: cavity and under-cavity sections (note that the cavity section can be considered and investigated as an independent model). Two metal side walls are attached to the cavity section by means of six bolts, thus simulating real car's door suspension. The under-cavity part includes boot's and engine's sections, the latter one being represented by a plate joined to the under-cavity part by four bolts and springs, that can be considered as engine mounts. All model parts were built of metal sheets of 1 mm thickness and spot welded where necessary. Both parts can be joined together by bolts to form a more complex model that is of primary interest in this investigation. Detailed pictures of all model's parts can be seen in Fig. 1.

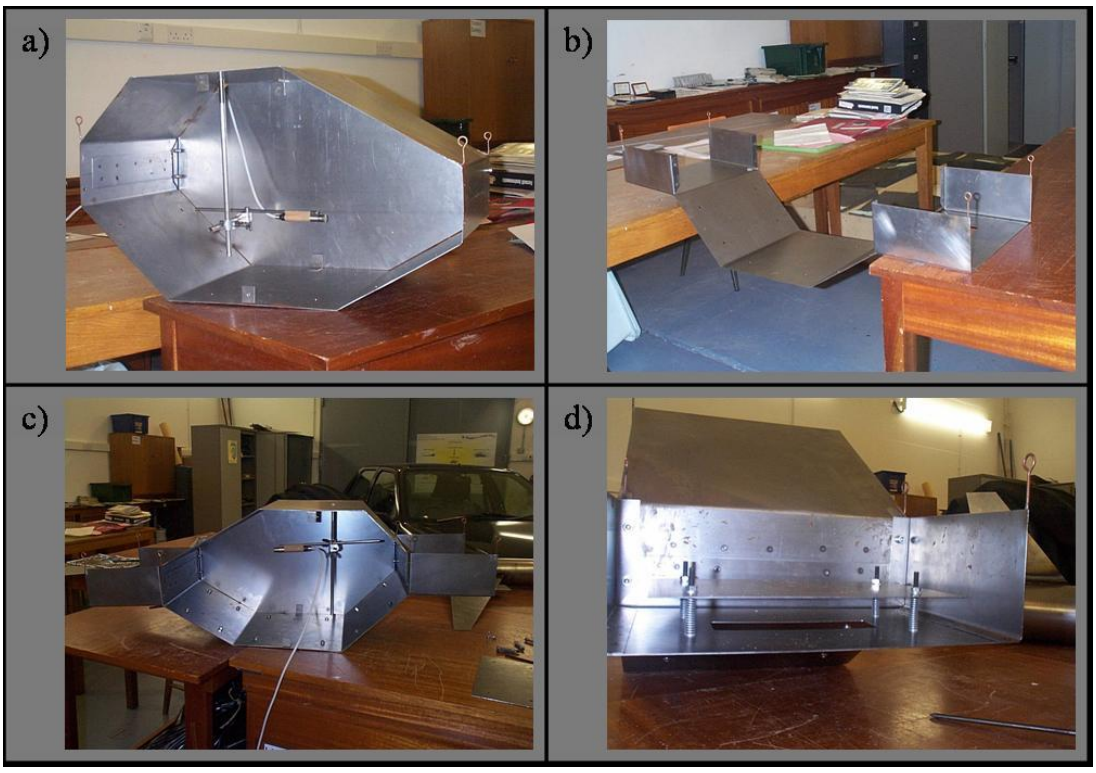

Figure 1. Detailed pictures of the model parts: a) cavity model, b) under-cavity section, c) whole model and d) engine section

In order to assure similar boundary conditions to real vehicles the model was fixed by four bolts to two wooden beams that in turn were firmly joined to a fundament by clamps. In this way, only four points of the model have constrains, and they enable a higher degree of freedom typical of real

cars. This attachment of the model corresponds to the so-called “grounded” boundary conditions. “Free-free” boundary conditions were also tested, but the resonant frequency of the system springs-model’s mass was not achieved to be away from the range of interest because of the limited choice of elastic (spring) elements.

All experimental measurements of structure-borne interior noise have been carried out in the Noise and Vibration Laboratory at the Department of Aeronautical and Automotive Engineering at Loughborough University. The measurement data were recorded using an HP 3566 FFT analyser. The excitation signal, a continuous white noise, was generated by the analyser and transmitted to a Ling Dynamic Systems 200 series electromagnetic shaker by means of an amplifier ENDEVCO Model 27218. The amplitude of the driving force from the shaker was measured using a sample mass and accelerometer, and was evaluated as 2.8 N. For acoustic frequency response measurements a Bruel&Kjaer Type 4133 microphone was used. Its signal was amplified by a Dual Microphone Supply Type 5935. A clamp enabling longitudinal and lateral motion inside the cavity assured the positioning of the microphone. The Bruel & Kjaer Type 2635 charge amplifier was used to enhance the signal from a force transducer Bruel & Kjaer Type 8200. The transducer’s reference sensitivity was 3.85 pc/N and it weighed 21g.

3 RESULTS AND DISCUSIONS

3.1 Structural-acoustic normal mode analysis

The structural-acoustic normal mode analysis has been conducted numerically using FEM for two different cases. In the first case, only the cavity model was considered, whereas in the second case the whole model, including the cavity plus under-cavity body, was under examination. For both models the interior cavity is the same, and the acoustic model for it was built using 3420 CHEXA and 44 CPENTA acoustic finite elements and in total 4147 nodes. The structural model of the cavity itself was constructed using 1342 CQUAD structural finite elements and 1458 nodes. The whole structural model consists of 1662 CQUAD structural elements and 1863 nodes. The normal mode analysis was performed using modal analysis reduction for the first 300 modes only. In contrast to the model presented in Ref. [14], the present two models have higher numbers of degrees of freedom. There are about 293 natural frequencies in the range from 0 to 1.7 kHz.

The normal modes of the first model include local modes from the individual panels and global ones, which spread almost over all panels. The analysis shows that the structure can not be broken up into different regions in specific frequency ranges, as it was possible for QUASICAR model [14,] because constitutive panels have nearly the same modal parameters and their natural frequencies exist in the whole frequency range. However, the side walls demonstrate some more specific vibration behaviour because of the particular way of their attachment to the main structure, which presumes less restrictions compared to other panels. Most of their normal modes can be defined as local. The participation of side walls’ normal modes in global structural displacement of the model can be hardly observed at certain frequencies.

In contrast to the side walls, the main structure exhibits more complex and obscure vibration behaviour, as it can be seen in Fig. 2. The constitutive panels take part in the global and local structural displacement. In the low frequency range the global modes are predominant, whereas in the high frequency range the local modes of different panels become readily distinguishable. An interesting point about the current model is the effect of absence of simply supported boundary conditions along edges of the main structure, which facilitates the global modes to appear at very low frequency, as it can be seen in Fig. 2 (d). Note that the global modes of the QUASICAR model (with simply supported boundary conditions along the structure’s edges) appeared at high frequency, above 1 kHz. Thus, one can conclude that the presence of simply supported boundary conditions along plate’s longitudinal edges emphasize the effect of transversal edges which separate the individual panels. Thus, the local modes for each panel could be successfully approximated by modes of the plates with simply supported boundary conditions, as it was shown in

Ref. [14]. Contrarily, the absence of simply supported boundary conditions along longitudinal edges lessens the effect of transversal edges and a structure could not be separated into its compound panels.

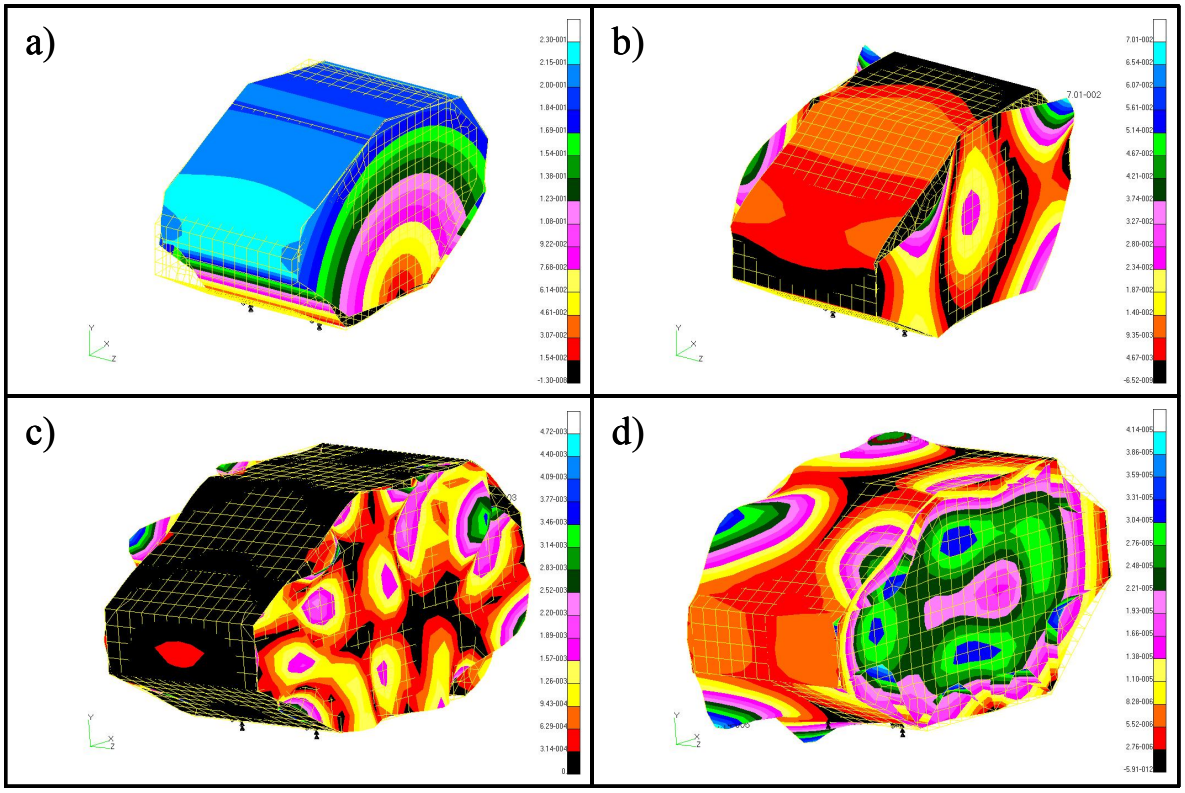

Figure 2. Normal modes of the cavity model at different resonant frequencies: a) 11.525 Hz, b) 59.586 Hz, c) 325.07 Hz and d) 560.65 Hz

The structural-acoustic normal mode analysis of the whole model, including cavity plus under-cavity body, shows some resemblance to the first model, but demonstrates certain specific features as well. Again, in this case the side walls are involved in many normal modes in the whole frequency region. The structural behaviour is affected by boot and engine sections which are firmly jointed to the cavity and side walls by bolts. This is why, the first resonant peak for this model exists at a higher frequency, 21.87 Hz, whereas in the first model the fundamental frequency is 11.525 Hz (see Fig. 2 (a), Fig. 3 (a) and Table 1). The boot and engine sections, particularly their vertical sides, appear to be quite loose; they are first involved in the normal mode at 42 Hz (see Fig. 3 (b)) and stay active in the whole frequency range. The surface displacements of the upper three cavity's panels look similar to the first model (i.e. see Fig. 2 (d) and Fig. 3 (e)), but the global modes which they are involved in are realized at higher frequencies (Fig. 3 (e) and (f)) compared to the cavity model only. The reason for that could be the double thickness of the bottom cavity's panels due to adjoining the under-cavity body to the cavity.

The bottom cavity's panels, in case if the whole model is considered, have completely different modal parameters due to the double thickness and their surface displacements drastically differ compared to the first model. The fundamental local frequency for the bottom plate exists at 64.369 Hz in the first model and at 196.98 Hz in the second model. In the low and medium frequency ranges this part of the whole model is almost silent and its structural activity starts at higher frequencies. This behaviour could be likened to the modified QUASICAR model with increased thickness of the bottom panel [14]. In both cases the additional thickness suppressed structural

activity of the treated panels in certain frequency range. This is a simple demonstration of passive structural vibration control.

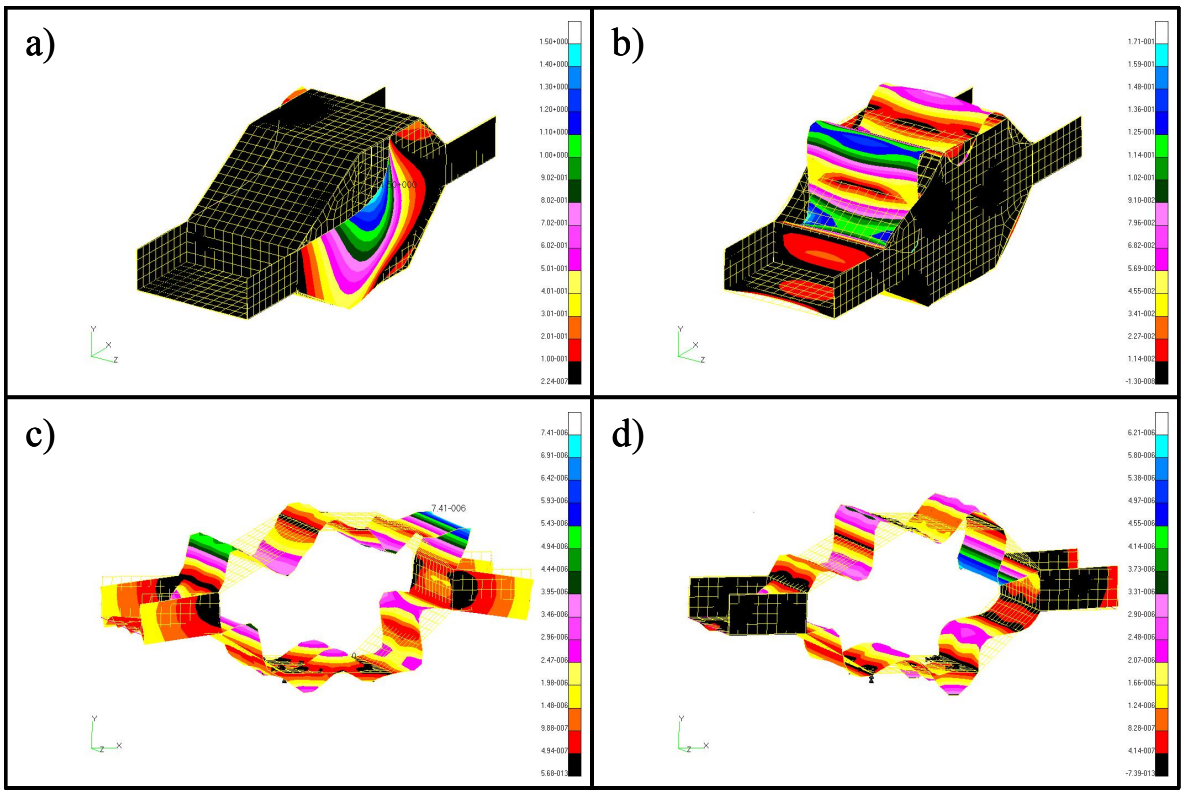

Figure 3. Normal modes of the whole model at different resonant frequencies: a) 21.87 Hz, b) 136.91 Hz, c) 1399.20 Hz and d) 1629.6 Hz

In Table 1, Columns 3, 4 and 5, one can see the values of the first five acoustic frequencies for the acoustic model with hard walls, for the cavity model and for the whole model respectively. The first four acoustic modes can be seen in Fig. 3. Obviously, the different boundary conditions for each model affect the acoustic resonance peaks of the cavity, shifting slightly their frequencies.

cavity model, str. freq., Hz	whole model, str. freq., Hz	acoustic freq. (hard walls), Hz	cavity model, acoustic freq., Hz	whole model, acoustic freq., Hz
1	2	3	4	5
11.525	21.87	326.66 (1, 0, 0)	325.07	327.51
15.52	28.759	529.22 (0, 1, 0)	536.00	538.44
23.486	31.498	553.74 (0, 0, 1)	560.65	555.18
26.626	33.28	584.46 (2, 0, 0)	589.45	588.24
28.255	36.394	642.92 (1, 0, 1)	648.76	646.53

Table 1. First five structural and acoustic natural frequencies of the cavity and of the whole model

Unfortunately, the observation of a set of acoustic resonances for these three models did not show a specific pattern, except for the resonant peaks of the latter two models that appear to be higher than those of the first one, as it can be seen in the table. Thus, one could not conclude how exactly the additional under-cavity body mass influences the acoustic normal modes of the cavity. However, the change in the frequency sets for the first case and the latter two is readily noticeable and reflects the structural-acoustic coupling.

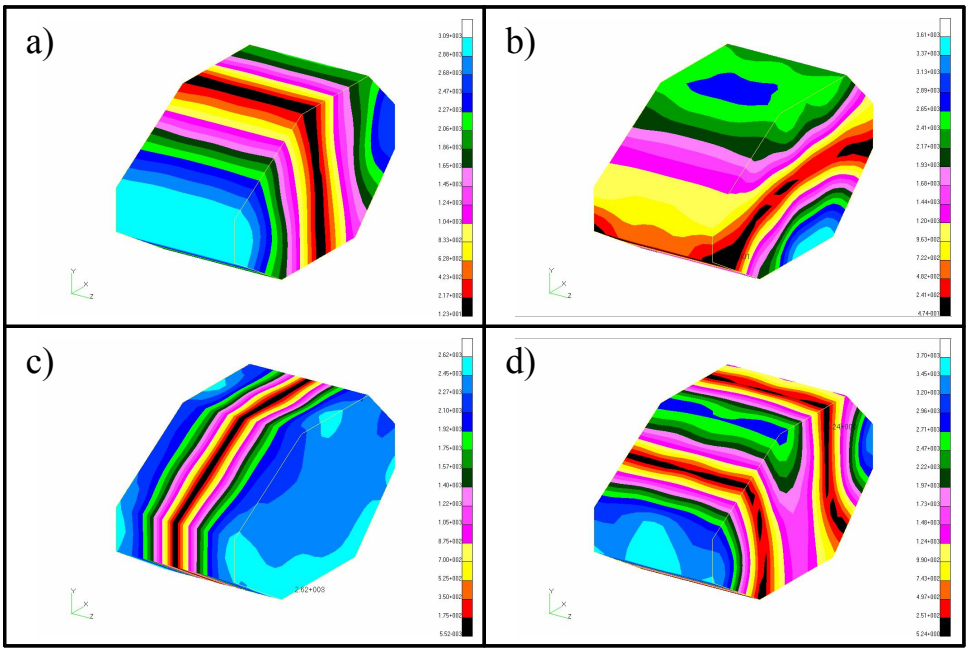

Figure 4. First four normal modes of the cavity interior at: a) 327.51 Hz b) 529.57 Hz c) 555.18 Hz d) 587.01 Hz

3.2 Frequency response analysis

The frequency response analyses have been conducted for both models using numerical and experimental techniques. In this section, 83 experimental tests and 48 numerical simulations have been carried out. The covered frequency range was between 0 and 1.6 kHz, which for full size models corresponds to the range 0 - 400 Hz. A resolution of one point per 1 Hz for both numerical and experimental tests was adopted. For all experimental tests the models were attached firmly to tables by using wooden beams mentioned in section 2. Because the masses of the tables were comparable to the masses of the models, the frequency response could be affected by tables' modal parameters. This is why heavy weights were placed on the top of the tables to assure proper grounded boundary conditions. The microphone was accommodated by a clamp fixed to the top panel, made of very light allow. Two points of the interior cavity were of particular interest, the driver's ear position (0, -90, 70) cm and the passenger's ear position (250, -90, 70) cm, with respect to the front upper left corner of the cavity.

3.2.1 Effect of different positions of the shaker and of the microphone

Both models have been examined in a number of structural-acoustic tests, including measurement of acoustic response at driver's and passenger's ear positions, when the electromagnetic shaker was located at five different positions. First of all, the locations of the shaker and of the microphone strongly influence the acoustic response. A simple explanation for this is that under the current conditions of relatively small driving forces both the structure and the fluid can be thought as linear systems which frequency responses can be represented as infinite sums of their normal modes.

If the driving force coincides with a certain nodal point of some structural normal modes, the structure will not be excited properly in their frequency ranges. The same situation can be considered for the location of a microphone. If the microphone (receiver) is located in the vicinity of a nodal point of some acoustic normal modes, then the sound pressure response will be reduced in

their frequency ranges. Thus, the location of the driving force and of the microphone could be used for optimal reduction of perceived interior noise.

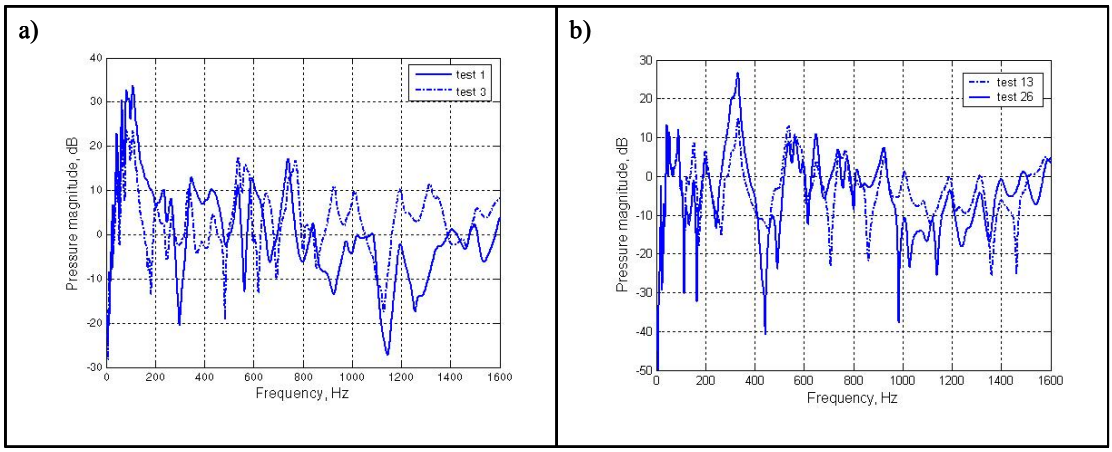

Figure 5. Numerically calculated effect of different locations of the driving force and of the microphone: a) driving force – central position, test 1 (solid curve) and left front position, test 3 (dash-dotted curve); and b) microphone – driver's, test 13 (dash-dotted curve) and passenger's, test 26 (solid curve) ear position

However, the practical effect of such an approach is arguable. The location of the driving force or of the microphone might coincide with nodal positions for some modes but also it might coincide with anti-nodal positions for some other normal modes. This means that the reduction can exist at certain frequency range, but at some others there can be an increase. Fig. 5 (a) shows the results of finite element calculations of the effects of different locations of the driving force of 2.8 N on the acoustic responses. Obviously, one can note that in test 3 the force can not excite properly some of the first normal modes. This is why in the low frequency range the acoustic response is reduced in comparison to test 1. On the other hand, in the high frequency range the location of driving force at the left front position disturbs the normal modes in this area and the acoustic response is higher than that in test 1. Fig. 5 (b) presents the acoustic responses at driver's (test 13) and passenger's (test26) ear positions taken from the whole model when the driving force was located at the left front position of the bottom plate. Similarly to the analysis above, the sound pressure readings shows some frequencies where the resonant peaks are reduced considerably, as at 320 Hz. In this case the sound perception at the driver's ear position is reduced almost by 10 dB compared to the passenger's ear position. However, at 1000 Hz the reduction is again 10 dB, but in favour of the passenger's ear.

3.2.2 Effect of engine and boot masses

The effect of additional masses placed in the engine's and boot's sections has been examined in experimental tests 57 to 75. For all of the tests the microphone was located at driver's ear position and the electromechanical shaker was shifted to different positions from left to right in engine's and boot's sections. However, no matter where the position of the shaker was, the sound pressure responses show some common features for all tests. As the engine's mass was separated from the main structure by elastic elements its effect on acoustic response was barely detectable, as it can be seen in Fig. 6 (a). The graphs show the pressure magnitude without engine's mass (test 66) and with engine's mass equal to 5 lb (test 67), when the shaker was placed at the middle left position of boot's plate. Thus, the existence of elastic elements between the engine's mass and the structure simulated engine's mounts and their influence on interior noise. Although the resulting tests pointed out clearly that the elastic elements suppresed successfully the effects of engine's mass, it must be

mentioned that the engine was simulated only as a mass unit. However, in practice engine disturbs car structure through its own vibrations, which requires a special consideration.

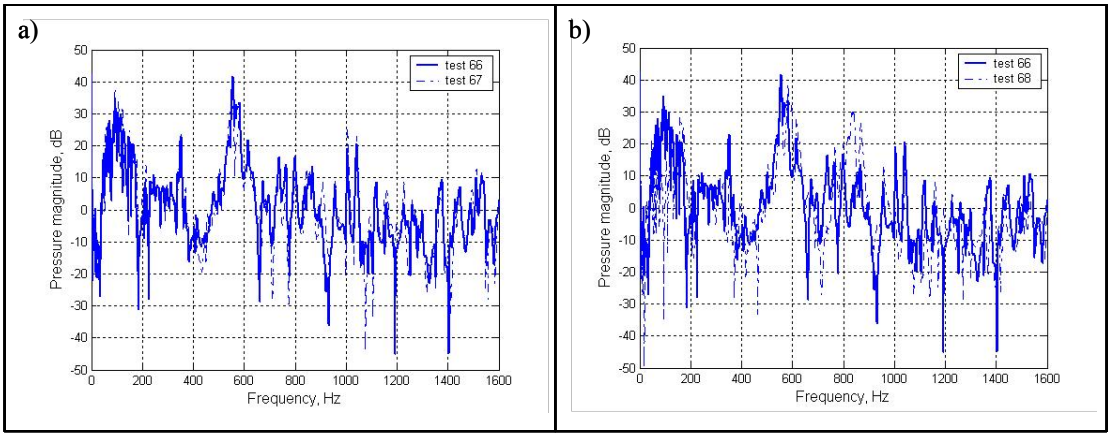

Figure 6. Effects of engine and boot masses: a) engine mass: no engine mass, test 66 (solid curve) and with engine mass, test 67 (dash-dotted curve); b) boot mass – no boot mass, test 66 (solid curve) and with boot mass, test 68 (dash-dotted curve)

Figure 6 (b) shows the graphs of sound pressure response without mass in the boot's section (test 66) and with boot's mass equal to 5 lb (test 68). In contrast to engine's attachment, the boot's mass was placed freely in the boot's section without any elastic elements, which creates more distinctive results compared to the original model. If the resonant peaks are not shifted in Fig. 6 (a) due to the elastic elements, in Fig. 6 (b) the natural frequencies are slightly shifted and also there are some changes in their amplitudes. Particularly, in the low frequency range the maximum peak is shifted at about 90 Hz to 160 Hz and the sound response behaviour below this peak is somewhat suppressed. In the high frequency range, above 1 kHz, the acoustic response is slightly reduced. Although the overall sound levels in case of boot mass remain aproximately the same, the experiments demonstrate the influence of additional masses in the form of luggage in the boot's section. Sometimes such an exseptional load could cause a rather high resonance peak at certain frequency, which could annoy the driver and passengers in the compartment. Such a peak can be observed in Fig. 6 (b) between 800 and 900 Hz.

Figure 7 presents the results for acoustic response in the case when the electromagnetic shaker was attached directly to the engine's plate. Test 70 corresponds to the experiment with elastic elements, whereas test 74 is without springs, and the engine's plate is firmly joined to the main structure. Now the effect of elastic elements is clearly seen. In the range between 250 and 350, 650 – 750 and 1200 - 1400 Hz, one can see a considerable reduction of sound pressure. In this case the elastic elements successfully dissipate the vibrational energy going through them to the main structure. In other frequency areas, such as 0 – 200 and 900 – 1000 Hz, elastic elements act as an amplifier and enhance the

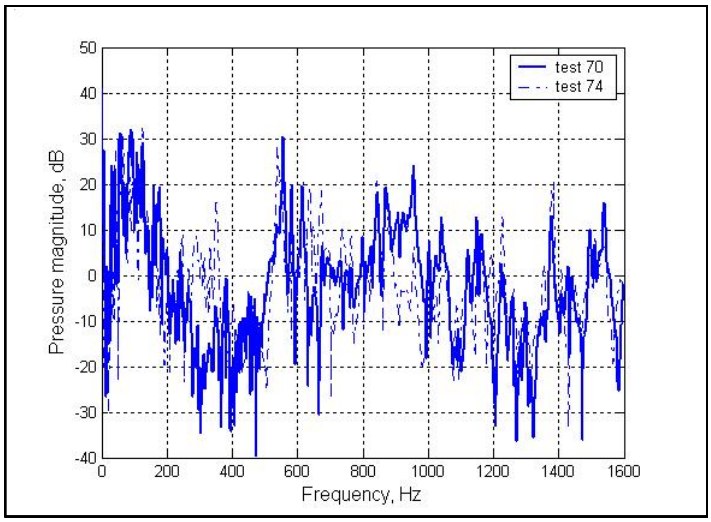

Figure 7. Effect of elastic suspension of the engine: test 70 (solid curve) – with elastic elements, and test 74 (dash-dotted curve) - without elastic elements

disturbance passing through them. Therefore, as was mentioned above, the calculation of engine's mounts must be done for specified frequency ranges.

3.2.3 Comparison between experimental and finite element data

The purpose for comparing experimental and finite element data in the present research is just to evaluate to what extent the proposed experimental and numerical approaches are reliable and precise. Fig. 8 shows sound pressure responses for experimental and finite element simulations for the whole model. The electromagnetic shaker with the force amplitude of 2.8 N was placed in a front right position to the engine's section (Fig. 8 (a)) and in a back right position to the boot's section (Fig. 8 (b)). Finite element mesh was consistent with the frequency limit of interest about 500 Hz; with about six finite elements per wavelength. In the FEM frequency response analysis, a resolution equal to one point per 1 Hz was used, which was the same as in the experimental testing.

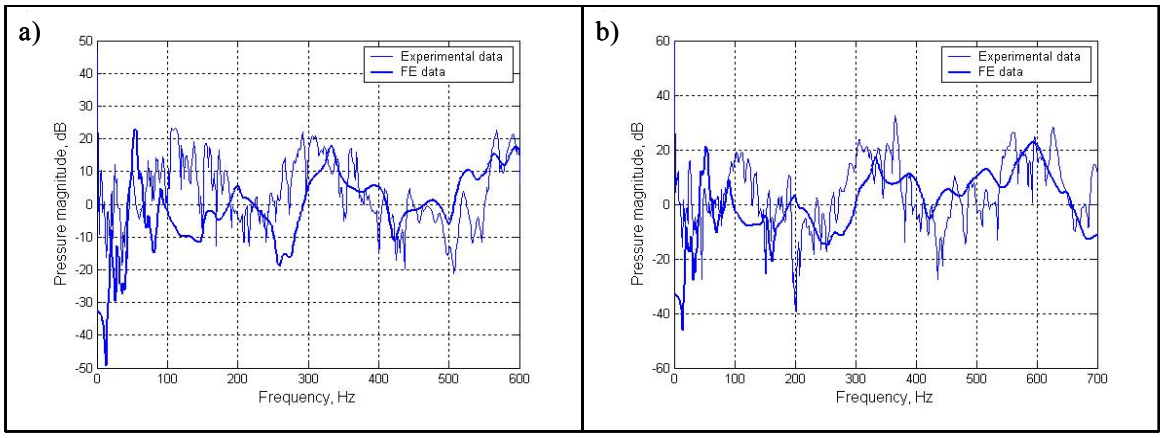

Figure 8. Comparison between FEM calculations (doubled thickness curves) and experimental measurements (single thickness curves)

Although there is a very good overall coincidence between experimental and FEM data, there is a number of disagreements, particularly in the frequency range between 100 and 200 Hz. Obviously, the experimental model has more natural frequencies than the FEM model and there are a number of resonant peaks that have not been predicted by the FEM software. The most likely reason for that could be the smaller number of degrees of freedom in the FEM model compared to the experimental model. In the numerical simulations, approximately 1800 structural and 4000 acoustic nodes were used which is not comparable with the endless numbers of them in the real models. However, as was mentioned above there is a good overall coincidence of the acoustic responses, which proves the FEM approach as precise and reliable enough for conducting primary analysis, where a lot of simulations are required to estimate the effects of all design parameters. The use of simplified models at this stage could help, accelerate and decrease the price of FEM analysis.

4 CONCLUSIONS

In the present paper, the results of experimental and numerical studies of structure-borne interior noise in two simplified vehicle models have been reported. In particular, the normal mode analysis of the models and of their frequency responses has been carried out using finite element simulations. A large number of experimental tests have been conducted. Some of them have been compared to the results following from finite element simulations. The normal mode analysis of both models showed that the natural frequencies of their constitutive panels lie in the same frequency range and the natural frequencies of the models can not be divided into groups and approximated

by the corresponding panels. Also, it was pointed out that the absence of simply-supported boundary conditions along the longitudinal edges lessens the effect of transversal edges which assists the global normal modes to appear at lower frequencies.

Using frequency response analysis, the effects of various factors were evaluated and demonstrated. First of all, it was shown that the positions of the driving force and of the microphone change significantly the sound pressure response in cases when they are placed at a node or anti-node of respective structural or acoustic normal modes. It has been also demonstrated that the effect of engine mass could be significant or negligible depending on the elastic elements, whereas the boot's mass could create unexpected resonance peak at certain frequency. Some useful measures of the interior noise reduction have been discussed.

The main idea promoted in this paper is usefulness of the analysis of vehicle interior noise using simplified reduced-scale vehicle models that are more complex than a rectangular box with one flexible wall, but still simple enough to be understandable. In this way, such simplified models can bridge the existing gap between the simplest analytical models and the modern commercial computer models used in automobile industry. The confirmation of usefulness of this phylosophy is the good agreement between experimental and numerical data demonstrated in this paper.

5 REFERENCES

1. M. Pozar, H.E. Cook: On determining the relationship between vehicle value and interior noise. SAE 980621 (1998) International Congress & Exposition, Detroit, MI.
2. R. Bisping, S. Giehl, M. Vogt: A standardised scale for the assessment of car interior sound quality. SAE 971976 (1997).
3. A.J. Pretlove: Free vibrations of a rectangular panel backed by a closed rectangular cavity. Journal of Sound and Vibration, 2 (1965), 197-209.
4. A.J. Pretlove, Forced vibrations of a rectangular panel backed by a closed rectangular cavity. Journal of Sound and Vibration, 3 (1966), 252-261.
5. R.H. Lyon: Noise reduction of rectangular enclosures with one flexible wall, J. Acoust. Soc. Am., 35 (1963), pp 1791-1797.
6. T.C. Lim: Automotive panel noise contribution modelling based on finite element and measured structural-acoustic spectra. Applied Acoustics **60** (2000) 505-519.
7. D.J Nefske, J.A. Wolf Jr, L.J. Howell: Structural-acoustic finite element analysis of the automobile passenger compartment: a review of current practice. Journal of Sound and Vibration **80** (1982) 247-266.
8. S.H. Sung, D.J. Nefske: A coupled structural-acoustic finite element model for vehicle interior noise analysis, J. Vibr., Acoust., Stress, Relaib. Design, Trans. of the ASME, 106 (1984), pp 314-318.
9. W.G. Lee, S.K. Park, M.W. Suh: A study on active noise control using the half scaled compartment cavity model. SAE 940606 (1994).
10. R. Gorman, V.V. Krylov: Investigation of acoustic properties of vehicle compartments using reduced-scale simplified models. Proceedings of the Institute of Acoustics **26** (2004) 37-48.
11. R. Rashid, R.S. Langley: A hybrid method for modelling in-vehicle boom noise. Proceedings of ISMA Prague (2004) 3487-3500.
12. V.V. Krylov: Simplified analytical models for prediction of vehicle interior noise. Proceedings of the International Conference on Noise and Vibration Engineering ISMA Belgium **5** (2002) 1973-1980.
13. V.V. Krylov, S.J. Walsh, and R.E.T.B. Winward: Modelling of vehicle interior noise at reduced scale, Proceedings of Euronoise 2003, Naples, 2003 (on CD).
14. V.B. Georgiev, V.V. Krylov and R.E.T.B. Winward: Finite element analysis of structural-acoustic interaction in simplified models of road vehicles, Proceedings of the Institute of Acoustics, Southampton, Vol. 26, Pt. 2, 2004 (on CD).